A remotely interrogated all-optical ^{87}Rb magnetometer

B. Patton,[1,a)] O. O. Versolato,[2,b)] D. C. Hovde,[3] E. Corsini,[1] J. M. Higbie,[4] and D. Budker[1,5]

[1]*Department of Physics, University of California, Berkeley, California 94720-7300, USA*
[2]*Kernfysisch Versneller Instituut, University of Groningen, NL-9747 AA Groningen, The Netherlands*
[3]*Southwest Sciences, Inc., Cincinnati, Ohio 45244, USA*
[4]*Department of Physics and Astronomy, Bucknell University, Lewisburg, Pennsylvania 17837, USA*
[5]*Nuclear Science Division, Lawrence Berkeley National Laboratory, Berkeley, California 94720, USA*

Atomic magnetometry was performed at Earth's magnetic field over a free-space distance of ten meters. Two laser beams aimed at a distant alkali-vapor cell excited and detected the ^{87}Rb magnetic resonance, allowing the magnetic field within the cell to be interrogated remotely. Operated as a driven oscillator, the magnetometer measured the geomagnetic field with $\lesssim 3.5$ pT precision in a ~ 2 s data acquisition; this precision was likely limited by ambient field fluctuations. The sensor was also operated in self-oscillating mode with a 5.3 pT$/\sqrt{\text{Hz}}$ noise floor. Further optimization will yield a high-bandwidth, fully remote magnetometer with sub-pT sensitivity. © *2012 American Institute of Physics*. [http://dx.doi.org/10.1063/1.4747206]

Shortly after the inception of atomic magnetometry, alkali-vapor magnetometers were being used to measure the Earth's magnetic field to unprecedented precision. During the same era, Bell and Bloom demonstrated all-optical atomic magnetometry through synchronous optical pumping.[1] In this approach, optical-pumping light is frequency- or amplitude-modulated at harmonics of the Larmor frequency ω_L to generate a precessing spin polarization within an alkali vapor at finite magnetic field. Although this technique received considerable attention from the atomic physics community for its applicability to optical pumping experiments, Earth's-field alkali-vapor atomic magnetometers continued to rely on radio frequency (RF) field excitation for several decades. Upon the advent of diode lasers at suitable wavelengths, synchronously pumped magnetometers experienced a revival beginning the late 1980s. In recent years, advances in all-optical magnetometers using amplitude-modulated[2] and frequency-modulated[3] light have resulted in applications such as nuclear magnetic resonance detection,[4] quantum control experiments,[5] and chip-scale devices intended for spacecraft use.[6]

All-optical magnetometers possess several advantages over devices which employ RF coils. RF-driven magnetometers can suffer from cross-talk if two sensors are placed in close proximity, since the AC magnetic field driving resonance in one vapor cell can adversely affect the other. All-optical magnetometers are free from such interference. When operated in self-oscillating mode,[7] RF-driven magnetometers require an added $\pm 90^\circ$ electronic phase shift in the feedback loop to counter the intrinsic phase shift between the RF field and the probe-beam modulation. In an all-optical magnetometer, this same phase shift can be achieved simply by varying the relative orientations of the pump and probe beam polarizations.[8] Most importantly, all-optical magnetometers require no physical connection between the driving electronics and the alkali-vapor cell. This allows completely remote interrogation of the magnetic resonance in a faraway atomic sample. Here, we describe a demonstration of remotely interrogated all-optical magnetometry.

A schematic of the remote-detection magnetometer is shown in Fig. 1. The unshielded sensor was similar to that described in Ref. 8 in that the pump and probe beams were derived from a single laser whose frequency was stabilized by a dichroic atomic vapor laser lock (DAVLL).[9] The atomic sample consisted of an antirelaxation-coated[10] alkali-vapor cell containing enriched ^{87}Rb and no buffer gas; the longitudinal spin relaxation time of atoms within the cell was 1.2 s. The laser beams were carried from an optics and electronics rack to a launcher assembly via polarization-maintaining optical fibers; the pump beam amplitude was modulated with a fiberized Mach-Zender electro-optic modulator (EOM). At the launcher, the collimated output beams were linearly polarized and aimed at a sensor head placed 10 m away. This assembly contained the ^{87}Rb cell within an enclosure heated to 34.5 °C by a 1.7 kHz alternating current flowing through counter-wrapped heating wires. These wires comprised the only physical contact between the experimental apparatus and the atomic sample. In principle, such heating is not necessary, but it was employed here to boost the optical-rotation signal above electronic interference from AM radio stations.

The probe beam traveled horizontally through the optical cell in a double-pass configuration, reflecting off a mirror behind the cell and propagating back toward the launcher. There, a balanced polarimeter split the probe beam into orthogonal polarizations which were projected onto two photodiodes, allowing optical rotation to be measured. Synchronous optical pumping at $2\omega_L$ created atomic alignment[11,12] within the ^{87}Rb vapor which produced time-varying optical rotation of the probe polarization at ω_L and $2\omega_L$. The ω_L harmonic arises when the field is tilted away from the direction of the probe beam propagation vector.[13] In the current experiment, the ambient geomagnetic field pointed 32° from the vertical, leading to an optical rotation component at ω_L which was several times larger than the $2\omega_L$ harmonic. Note that this field orientation is far from optimal, since both harmonics exhibit zero amplitude when

a)Electronic mail: bpatton@berkeley.edu.
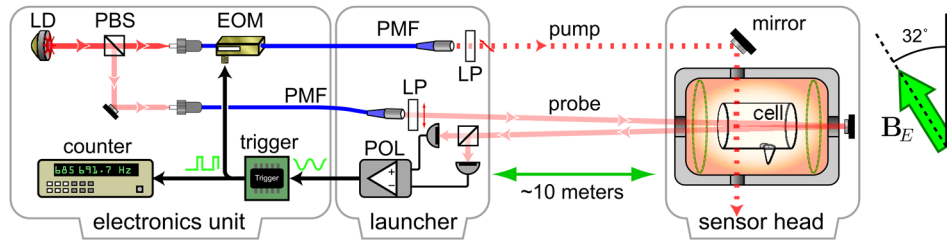b)Present address: Max-Planck-Institut für Kernphysik, Heidelberg, Germany.

FIG. 1. Schematic of the remote-detection magnetometer. The laser diode (LD) beam was split with a polarizing beamsplitter (PBS) and coupled into two polarization-maintaining fibers (PMF). The pump beam amplitude was modulated by a fiberized EOM. At the launcher, both beams were collimated, sent through linear polarizers (LP), and aimed at the sensor head. The pump beam was polarized horizontally, creating atomic alignment perpendicular to the ambient field. The probe beam reflected off a mirror aimed at a balanced polarimeter (POL) within the launcher. In self-oscillating mode (depicted), the polarimeter output was conditioned to drive the EOM directly. In driven-oscillation mode, the EOM was driven by a swept frequency source and the polarimeter output demodulated with a lock-in amplifier. The Earth's field $\mathbf{B}_E$ was independently measured to be 32° from the vertical in the direction depicted.

the magnetic field is perpendicular to the probe beam propagation[13] (a configuration known as a "dead zone").

The Zeeman shifts of the alkali ground-state sublevels (total electron spin $J = 1/2$) at a magnetic field B can be calculated from the Breit-Rabi equation.[14]

$$E(F, m_F) = -\frac{\mathcal{A}_{\text{hfs}}}{4} - g_I \mu_B m_F B$$
$$\pm \frac{\mathcal{A}_{\text{hfs}}(I + \frac{1}{2})}{2} \sqrt{1 + \frac{4m_F x}{2I + 1} + x^2}, \quad (1)$$

where E is the energy of the ground state sublevel with quantum numbers F and m_F ($F = I \pm \frac{1}{2}$ being the total angular momentum of the ground state and I the nuclear spin), $\mathcal{A}_{\text{hfs}}$ is the hyperfine structure constant, and the perturbation parameter x is given by

$$x \equiv \frac{(g_J + g_I)\mu_B B}{\mathcal{A}_{\text{hfs}}(I + \frac{1}{2})}. \quad (2)$$

Here, g_J and g_I are the electron and nuclear g factors, respectively.[15] At low magnetic fields, a linear approximation to Eq. (1) predicts a single resonance at ω_L for all transitions with $\Delta m_F = 1$ and another resonance at $2\omega_L$ for all $\Delta m_F = 2$ transitions. At Earth's field (B_E), these resonances split into sets of resolved transitions due to higher-order corrections. In the present study, the laser was tuned to address the $F = 2$ ground-state hyperfine manifold of ^{87}Rb, yielding four resonances with $\Delta m_F = 1$ and three with $\Delta m_F = 2$. The magnetometer is nominally designed to probe $\Delta m_F = 2$ resonances in order to reduce systematic errors,[16] but in this study it could also be operated near ω_L due to the field configuration.

In driven-oscillation mode, a function generator was used to drive the EOM and the probe beam optical rotation was detected with a lock-in amplifier (SR844, Stanford Research Systems, Inc.). The modulation frequency was swept around $2\omega_L$ in order to map out the $\Delta m_F = 2$ magnetic-resonance curve, which was recorded on an oscilloscope. An example data set is shown in Fig. 2. For these data, the pump beam power was set to 260 μW peak with a 50% duty cycle and the probe beam was 55 μW continuous. Three resonances separated by the ~70 Hz nonlinear Zeeman splitting are clearly visible.

Due to electrical interference, a phase-coherent signal was picked up by the lock-in amplifier; this produced a frequency-dependent offset even when the pump and probe

beams were blocked. This spurious baseline was subtracted from the data in Fig. 2 and the data were fit to the three-Lorentzian magnetic-resonance spectrum predicted by Eq. (1). According to this fit, the central ($m_F = -1 \rightarrow m_F = +1$) magnetic resonance occurs at 682 504.318 ± 0.050 Hz (1σ uncertainty). Converting the best-fit frequency uncertainty into a field uncertainty yields a magnetic sensitivity of 3.5 pT. The lock-in time constant was 10 ms and the frequency sweep rate was 200 Hz/s, such that most of the spectrum was recorded within a span of ~2 s. For the fitting procedure, the data were averaged in 10 ms bins in order to reduce correlations in point-to-point noise which would erroneously reduce the estimated frequency uncertainty. As a cross-check of this sensitivity figure, many sets of simulated data were generated with random noise which was statistically equivalent to the off-resonant noise measured in the experiment. Repeated least-squares fitting of this simulated data yielded a root-mean-square scatter of 0.046 Hz in best-fit frequency (equivalent to 3.3 pT) when all other fitting parameters were held fixed. The off-resonant noise indicates that if the EOM driving frequency was set to the zero-crossing of the dispersive trace shown in Fig. 2 and a steady-state experiment performed, fluctuations of ≳9.6 pT could be detected with a 1 Hz noise bandwidth.

This magnetometric sensitivity was achieved in spite of several sub-optimal experimental conditions: high pump and probe beam powers, excessive pump duty cycle, analog data transmission, and sub-optimal field orientation.[17] In a reference sensor consisting of identical components interrogated
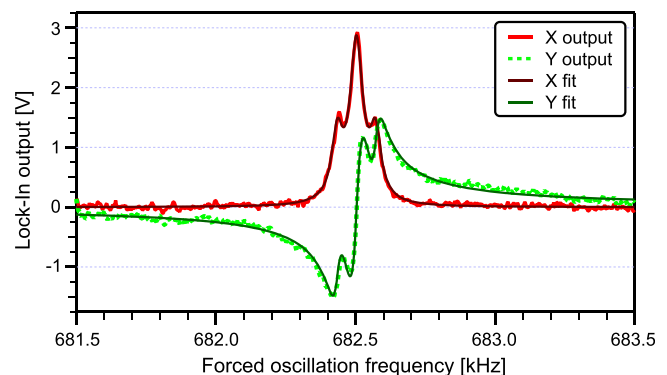

FIG. 2. Driven-oscillation data recorded with the remote magnetometer. A spurious background has been subtracted from the data, which were then fit to the spectrum predicted by Eq. (1). The data and the fit have been rephased to portray purely absorptive and dispersive quadratures.

non-remotely,[18] optimization of the pump power and duty cycle yielded an optical rotation signal 14 times larger than that shown in Fig. 2. This implies that optimization of the pump beam characteristics could immediately yield sub-pT sensitivity in the remote scheme. Moreover, these signals were recorded in an unshielded environment and subject to fluctuations in the ambient field which were often larger than 10 pT/s. Most likely, the sensitivity demonstrated here is limited by genuine field fluctuations. Improved sensitivities can therefore be expected in future experiments, particularly if a gradiometric scheme is employed.

In self-oscillating mode, the polarimeter output was conditioned by a triggering circuit to drive the EOM directly, generating a positive feedback loop and causing the system to oscillate spontaneously at the magnetic-resonance frequency. A passive band-pass filter of width 10 kHz centered around ω_L was included in the loop to reduce broadband noise fed into the triggering circuit. (Oscillation at $2\omega_L$ was also possible, but less robust due to AM radio interference and the smaller signal amplitude.) The probe beam power was 50 μW leaving the launcher; the pump beam power was 10 μW time-averaged with a low (10%-20%) duty cycle. To quantify the magnetometer's performance, we mixed down its self-oscillation signal with that of the reference sensor using the lock-in amplifier, with the reference sensor acting as the external frequency reference and the remote sensor as the signal input. Helmholtz coils near the test sensor generated a field offset seen by the two magnetometers. This gradient was tuned to generate a self-oscillation beat frequency of ∼275 Hz and the lock-in time constant set to 1 ms. The output of the lock-in amplifier was recorded with a data acquisition card and saved to a computer.

Figure 3 shows an analysis of the magnetic-field noise observed by the sensors. The SR844 output was digitally filtered with a 125 Hz band-pass filter about the intermediate frequency, then fit with a running sine wave in 8 ms segments to calculate the beat frequency as a function of time. This frequency was then converted into a fluctuation about Earth's field using Eq. (1), assuming that both magnetometers were oscillating on the same $\Delta m_F = 1$ resonance.[19] A Fourier transform of the field difference yielded the power spectral density (PSD) of the reported magnetic noise. The average noise floor from 1 Hz

to 50 Hz was 5.3 pT/$\sqrt{\text{Hz}}$. It is not clear how much of the PSD noise floor arises from sensor noise and how much can be attributed to current noise in the power supply driving the Helmholtz coils or fluctuations in the ambient field gradient. A principal advantage of the self-oscillating scheme is its high bandwidth—AC magnetic fields of frequency ≳1 kHz and magnitude 1 nT have been detected with high signal-to-noise using a version of the reference sensor described here.

Although a flat mirror was used in these experiments, such a configuration is not practical for remote magnetometry because the mirror must be aligned at the cell in order to reflect the probe beam back to the polarimeter. Replacing this mirror with a polarization-preserving retroreflector would allow for truly adjustment-free, long-baseline magnetometry. Corner-cube reflectors can significantly alter the polarization properties of an interrogating laser. An omnidirectional retro-reflecting sphere is a promising choice, with a graded-index Luneberg-like sphere being ideal. Polarimetry tests were conducted using a surrogate 1 cm diameter sphere with index of refraction $n \approx 2$, silver coated on its distal surface. Initial tests using a 633 nm laser and a digital polarimeter showed that the retroreflector (O'Hara Corp.) preserved linear polarization of a probe beam to within a few degrees of ellipticity, which represented the measurement error of the polarimeter. Future tests will incorporate this retroreflector in the magnetometer design. In addition, the free-space baseline of the magnetometer will be increased, with the expectation that this technique can be extended to distances of several hundred meters before atmospheric seeing becomes a significant noise source.[20] Beyond this distance scale, adaptive optics techniques may become necessary to mitigate the effects of atmospheric turbulence and retain magnetometric sensitivity.

A sensitive remote magnetometer capable of being interrogated over several kilometers of free space would be highly desirable in several applications, including ordnance detection, perimeter monitoring, and geophysical surveys. Inexpensive manufacturing of the cell/retroreflector package would allow many such sensors to be widely distributed and interrogated by a single optical setup. Further research in remote magnetometry will also contribute to recently proposed efforts to measure the Earth's magnetic field using mesospheric sodium atoms and laser guide-star technology.[21]
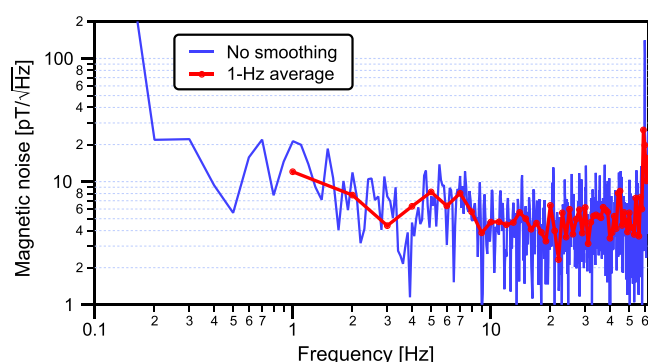
FIG. 3. PSD of the gradiometer signal. The beat frequency of the sensors was calculated as a function of time, converted into a field difference, and Fourier transformed to yield the magnetic noise as a function of frequency. The thin blue trace is the Fourier transform; the thicker red trace is the same data smoothed into 1 Hz bins. The mean noise floor between 1 Hz and 50 Hz is 5.3 pT/$\sqrt{\text{Hz}}$. Ambient 60-Hz magnetic field noise can be clearly seen.

[1]W. E. Bell and A. L. Bloom, Phys. Rev. Lett. **6**, 280 (1961).

[2]W. Gawlik, L. Krzemien, S. Pustelny, D. Sangla, J. Zachorowski, M. Graf, A. O. Sushkov, and D. Budker, Appl. Phys. Lett. **88**, 131108 (2006).

[3]V. Acosta, M. P. Ledbetter, S. M. Rochester, D. Budker, D. F. J. Kimball, D. C. Hovde, W. Gawlik, S. Pustelny, J. Zachorowski, and V. V. Yash-chuk, Phys. Rev. A **73**, 053404 (2006).

[4]G. Bevilacqua, V. Biancalana, Y. Dancheva, and L. Moi, J. Magn. Reson. **201**, 222 (2009).

[5]S. Pustelny, M. Koczwara, L. Cincio, and W. Gawlik, Phys. Rev. A **83**, 043832 (2011).

[6]H. Korth, K. Strohbehn, F. Tejada, A. Andreou, S. McVeigh, J. Kitching, and S. Knappe, Johns Hopkins APL Tech. Dig. **28**, 248 (2010).

[7]A. L. Bloom, Appl. Opt. **1**, 61 (1962).

[8]J. M. Higbie, E. Corsini, and D. Budker, Rev. Sci. Instrum. **77**, 113106 (2006).

[9]V. V. Yashchuk, D. Budker, and J. R. Davis, Rev. Sci. Instrum. **71**, 341 (2000).

[10]M. V. Balabas, T. Karaulanov, M. P. Ledbetter, and D. Budker, Phys. Rev. Lett. **105**, 070801 (2010).

[11]V. V. Yashchuk, D. Budker, W. Gawlik, D. F. Kimball, Y. P. Malakyan, and S. M. Rochester, Phys. Rev. Lett. **90**, 253001 (2003).

[12]Optical pumping with circularly polarized light modulated at ω_L creates atomic *orientation*, a net magnetization within the vapor. Linearly polarized light modulated at $2\omega_L$ generates *alignment*, a preferred axis of polarization which can be viewed as a twofold-symmetric spin distribution. The former represents a coherence between states with $\Delta m_F = 1$; the latter a coherence between states with $\Delta m_F = 2$ (where the quantization axis is along $\mathbf{B}_E$).

[13]S. Pustelny, W. Gawlik, S. M. Rochester, D. F. J. Kimball, V. V. Yash-chuk, and D. Budker, Phys. Rev. A **74**, 063420–063424 (2006).

[14]M. Auzinsh, D. Budker, and S. M. Rochester, *Optically Polarized Atoms: Understanding Light-Atom Interactions*, 1st ed. (Oxford University Press, USA, 2010).

[15]Here, we employ the sign convention of g_I such that the nuclear magnetic moment μ_N is given by: $\mu_N = g_I \mu_B \mathbf{I}$.

[16]B. Patton, O. O. Versolato, D. C. Hovde, E. Corsini, J. M. Higbie, S. M. Rochester, and D. Budker, "Heading error of an alignment-based 87Rb magnetometer" (unpublished).

[17]The amplitude of the $2\omega_L$ harmonic would have been much larger if the pump and probe beams were aligned along the ambient magnetic field, but such freedom cannot be assumed in practical applications of a remotely interrogated magnetometer.

[18]E. Corsini, Ph.D. dissertation, Univeristy of California, Berkeley, 2012.

[19]The *relative* field fluctuation measurement does not have any substantial dependence upon which $\Delta m_F = 1$ resonance is chosen; this remains true even if different resonances are assumed for the two sensors.

[20]A. L. Buck, Appl. Opt. **6**, 703 (1967).

[21]J. M. Higbie, S. M. Rochester, B. Patton, R. Holzlohner, D. Bonaccini Calia, and D. Budker, Proc. Natl. Acad. Sci. **108**, 3522 (2011).